Improved Semi-empirical Model of Proton Exchange Membrane Fuel Cell Incorporating Fault Diagnostic Feature

Saad Saleem Khan, Hussain Shareef, *Member*, *IEEE*, and Ahmad Asrul Ibrahim

***Abstract*—The membrane water content of the proton exchange membrane fuel cell (PEMFC) is the most important feature required for water management of the PEMFC system. Any improper management of water in the fuel cell may lead to system faults. Among various faults, flooding and drying faults are the most frequent in the PEMFC systems. This paper presents a new dynamic semi-empirical model which requires only the load current and temperature of the PEMFC system as the input while providing output voltage and membrane water content as its major outputs. Unlike other PEMFC systems, the proposed dynamic model calculates the internal partial pressure of oxygen and hydrogen rather than using special internal sensors. Moreover, the membrane water content and internal resistances of PEMFC are modelled by incorporating the load current condition and temperature of the PEMFC system. The model parameters have been extracted by using a quantum lightening search algorithm as an optimization technique, and the performance is validated with experimental data obtained from the NEXA 1.2 kW PEMFC system. To further demonstrate the capability of the model in fault detection, the variation in membrane water content has been studied via the simulation. The proposed model could be efficiently used in prognostic and diagnosis systems of PEMFC fault.**

***Index Terms*—Proton exchange membrane fuel cell (PEMFC) fault, membrane water content, modelling, optimization, quantum lightening search algorithm.**

I. Introduction

THE fuel cells are electrochemical energy conversion devices that convert chemical energy to electrical energy. In recent years, fuel cell research has become a promising area as it is applied in automobiles, aircrafts, the power sector, and other miscellaneous industries. Proton exchange membrane fuel cell (PEMFC) is the most commonly-used type of fuel cell in almost all major applications because of its low cost, durability, and compactness. It has high power density, low operation temperature, and the best efficiency among all other fuel cell variants. However, there are many issues related to the massive utilization of PEMFC systems because of their high cost and short lifetime [1]-[3].

In the PEMFC system, the main fuel is hydrogen gas, which reacts with oxygen in the presence of a catalyst to produce water and electricity. The existence of water is necessary for the proper operation of a PEMFC system. This is because an appropriate hydration of the membrane in the PEMFC system is necessary for the effective transportation of ions. Under dry ambient conditions, external humidifiers may be required for hydration. On the other hand, in humid locations, external fans may be used for removing excess water [2], [4]-[6]. Therefore, the behavior of water content in the PEMFC system is very important to model and analyze the overall performance.

Mathematical modelling has been used to simulate the process of the PEMFC system in order to take the best measures to improve their performances. The mathematical modelling of PEMFCs is divided into two groups: mechanistic modelling and semi-empirical modelling [7]-[10]. Mechanistic modelling involves the modelling of a PEMFC system based on electrochemical/thermodynamic equations of the PEMFC system, while semi-empirical modelling consists of theoretical and empirical equations of the PEMFC system, which are validated by a series of experiments performed on a PEMFC system. Semi-empirical models are reported to show better results and are less complicated than mechanistic models, especially when considering all auxiliary systems of PEMFCs such as fans and humidifiers [7], [9], [11]-[15].

The semi-empirical models discussed in [10], [13], [14], [16]-[19] consider the water balance in a PEMFC stack system with the pressure of water and vapor in the design. Water imbalance may cause drying or flooding faults. The temperature of a PEMFC system is the key to extracting the water content of the PEMFC system. Detailed studies of water management and associated faults regarding water abundance and scarcity are presented in [2], [17].

Membrane drying may occur ① due to insufficient humidification, especially when provided with extremely dry reactant gases; ② at high PEMFC temperature when the water

Manuscript received: March 22, 2019; accepted: December 10, 2019. Date of CrossCheck: December 10, 2019. Date of online publication: September 3, 2020.

This work was supported by United Arab Emirates University (Emirates Centre for Energy and Environment Research) (No. 31R067).

S. S. Khan and H. Shareef (corresponding author) are with the Department of Electrical Engineering, College of Engineering, United Arab Emirates University, 15551 Al Ain, United Arab Emirates (e-mail: saad.khan@uaeu.ac.ae; shareef@uaeu.ac.ae).

A. A. Ibrahim is with the Department of Electrical, Electronic and Systems Engineering, Faculty of Engineering and Built Environment, Universiti Kebangsaan Malaysia, 43600 UKM Bangi, Selangor Darul Ehsan, Malaysia (e-mail: ahmadasrul@ukm.edu.my).

DOI: 10.35833/MPCE.2019.000179

formation is not compensated; and ③ at high temperature with a step increase of current leading to dehydration. The rise in the temperature of PEMFCs may cause drying faults, especially with a step increase in load. These faults may be temporary if a proper self-humidification system is present. However, in regular commercial PEMFC systems, drying may be prolonged and cause permanent damage [2]. PEMFC temperature can increase or decrease with a change in ambient temperature because the PEMFC temperature is highly dependent on ambient temperature, cooling system, and loading current [15], [20], [21].

The flooding fault is categorized into three groups: anode flooding, cathode flooding, and flow channels flooding. The main concerns are in anode and cathode flooding. The cathode is more prone to flood than the anode because water formation occurs at the cathode after the reaction of oxygen reduction. Cathode flooding occurs at high loading and low temperature, while anode flooding occurs at low loading and low temperature [2]. A significant drop in PEMFC temperature under any loading condition may lead to flooding faults for low, medium, and high loading current.

The most recent semi-empirical model presented in [13] is developed with the pressure of vapor and water as variables for obtaining the output voltage. However, the deficiency of the model in [13] is that the partial pressure of hydrogen in the fuel cell is measured with the help of sensors. In this paper, the model from [13] is improved, and the variations of the membrane water content are also studied as an indicator of drying and flooding faults due to abrupt increases of the load and increase/decrease in the temperature of PEMFC.

The parameters of the proposed model are optimized using quantum lightening search algorithm (QLSA), as the modifications in the model require parameter optimization that not only fits the experimental voltage but also accounts for the generality of the model. After the validation of the model, the temperature of the PEMFC is varied in the simulation for the same specific loading conditions as performed in the experiments. For the acceptability of the proposed model, the variation in membrane water content should match with the theatrical and experimental findings on PEMFCs [2]. The main contribution of this paper is the development of an appropriate PEMFC model for quick drying and flooding fault diagnosis.

The remainder of this paper is organized as follows. Section II presents the details of the semi-empirical model presented in [13], and the necessary modifications proposed in this paper are explained in Section III. Section IV provides the details of the experiments performed on a PEMFC stack system. Section V presents a brief discussion on the application of QLSA in parameter estimation of PEMFC model. Section VI illustrates the results and presents discussions demonstrating the capability of the model to diagnose drying and flooding faults. Section VII concludes this paper.

II. Improvement of Selected Semi-empirical Model

The most recent semi-empirical model was developed in 2018 [13]. The model considers the pressure of vapor and water to obtain the system output voltage. However, the deficiency in this model is that the partial pressure of hydrogen in the fuel cell is measured by the sensors [13]. Moreover, the electronic resistance in [13] is taken as constant, which may not be the case in general as the internal resistance depends on the temperature [23]. The internal resistances, especially the electronic and ionic resistances of PEMFC, are the key factors that depend on the temperature of PEMFC, the water content of PEMFC, and loading conditions in obtaining the output voltage.

The voltage of a PEMFC system is difficult to calculate due to various non-linear voltage drops in the system. Activation voltage drops and concentration voltage drops are non-linear, while an ohmic voltage drop is linear, as shown in Fig. 1 [13].

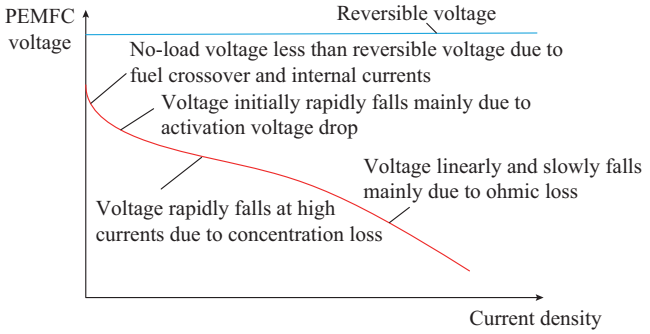

Fig. 1. PEMFC stack voltage against current density.

The total output voltage of a PEMFC system is given as:

$$V_{out} = V_{no,load} - V_{act} - V_{ohm} - V_{con} \tag{1}$$

where $V_{no,load}$ is the no-load or open circuit voltage; V_{act} is the activation voltage drop; V_{ohm} is the ohmic voltage drop; and V_{con} is the concentration voltage drop of the system. The model in [13] uses the Nernst equation for calculating the exchange membrane fuel (EMF) potential E_{cell} of a PEMFC system:

$$E_{cell} = E_{0,cell} + \frac{RT}{2F}\ln\left(\frac{P_{H2}P_{O2}^{0.5}}{P_{H2O}}\right) \tag{2}$$

where P_{H2} is the partial pressures of hydrogen; P_{O2} is the partial pressure of oxygen in ambient air; P_{H2O} is the pressure of water; T is the temperature of the PEMFC stack in Kelvin; R and F are gas constants with values 8.3143 $\mathrm{J\cdot mol^{-1}K^{-1}}$ and 96.487 $\mathrm{C\cdot mol^{-1}}$, respectively; and $E_{0,cell}$ is the reference potential, which is presented as:

$$E_{0,cell} = 1.229 - 8.5\times10^{-4}(T-298) \tag{3}$$

Usually, the pressure of water is ignored [14], since it is close to the unity for the temperature of PEMFC less than 373 K [13]. T is taken from sensors in the PEMFC system, while P_{H2} is also taken by internal sensors in [13].

Since a stack of PEMFC is the combination of n cells connected in series, the total EMF produced by stack E_{stack} is given as:

$$E_{stack} = nE_{cell} \tag{4}$$

The no-load voltage $V_{no,load}$ is less than EMF of the cells because of internal currents flowing through the circuit and a voltage drop produced, as shown in (5).

$$V_{no,load} = n\left[E_{0,cell} + \frac{RT}{2F}\ln\left(P_{H2}P_{O2}^{0.5}\right) - (V_{int} + V_{H2O})\right] \quad (5)$$

where V_{int} is the voltage drop due to internal currents; V_{H2O} is the voltage drop due to the pressure of water P_{H2O}; and $V_{int} + V_{H2O}$ is extracted using temperature T and P_{H2}.

$$n(V_{int} + V_{H2O}) = A_1 T P_{H2} + A_2 \quad (6)$$

where A_1 and A_2 are empirical expression constants, and are given as 0.0219 and 18.8223, respectively. T and P_{H2} are taken from the internal sensors of the NEXA 1.2 kW PEMFC system [13]. In most commercial PEMFC systems, these sensors are not available, and the applied pressure of hydrogen fuel P_{an} is known. The activated voltage drop is among the key voltage drops as:

$$V_{act} = \frac{RT}{2\alpha F}\ln\left(\frac{I}{i_o}\right) \quad I > i_o \quad (7)$$

where α is the charge transfer coefficient; I is the current; and i_o is the exchange current density given as:

$$i_o = B_1 F \exp\left(\frac{-1.229B_2F}{RT}\right) \quad (8)$$

where B_1 and B_2 are the coefficients. The ohmic voltage drop is given as:

$$V_{ohm} = I\left(R_{ionic} + R_e\right) \quad (9)$$

where R_{ionic} is the ionic resistance; and R_e is the electronic resistance. To calculate R_{ionic}, the relative humidity φ and membrane water content λ_m must be obtained.

$$\varphi = \frac{P_{H2O}}{P_{vap}} \quad (10)$$

where P_{vap} is the vapor pressure of PEMFC system. P_{vap} depends on the internal temperature of the PEMFC and is given by the following empirical formula:

$$\begin{aligned}\lg\left(P_{\text{vap}}(T)\right) = {} & 6.02724\times10^{-3} + 4.38484\times10^{-4}(T-273.15) + \\ & 1.39844\times10^{-5}(T-273.15)^2 + 2.71166\times10^{-7}(T-273.15)^3 + \\ & 2.57731\times10^{-9}(T-273.15)^4 + 2.82254\times(T-273.15)^5\end{aligned} \quad (11)$$

P_{H2O} is extracted by (6) using V_{H2O}, and V_{int} is 0.09 [13]. The equations for calculating P_{H2O} are as follows:

$$n(V_{H2O} + V_{int}) = nA_{H2O}T\ln\left(P_{H2O}\right) = A_1 T P_{H2} + A_2 \quad (12)$$

$$P_{H2O} = \exp\left(\frac{V_{H2O}}{TA_{H2O}}\right) \quad (13)$$

where A_{H2O} is the empirical expression constant for the pressure of water. After calculating the relative humidity from all the expressions given in (10)-(13), the membrane water content λ_m, which is the polynomial expression of relative humidity, is presented as:

$$\lambda_m = 0.043 + 17.81\varphi - 39.85\varphi^2 + 36\varphi^3 \quad (14)$$

The main purpose for calculating membrane water content λ_m is to calculate R_{ionic}, which is dependent on the current, temperature, and membrane water content of PEMFC:

$$R_{ionic} = \frac{C_1\left[1 + 0.03I + 0.062\left(\frac{T}{303}\right)^2 I^{2.5}\right]}{\left(\lambda_m - 0.634 - 3I\right)\exp\left(4.18\left(\frac{T-303}{T}\right)\right)} \quad (15)$$

where C_1 is a constant related to membrane thickness.

R_e is taken as constant in [13] for simplicity. However, in reality, it depends on electronic conductivity of the membrane and its thickness. The change in concentration voltage drop depends on the loading current. The concentration voltage V_{con} is obtained from [13] as:

$$V_{con} = \frac{-NRT}{2F}\ln\left(1 - \frac{I}{I_{lim}}\right) \quad (16)$$

where N is the population size; and I_{lim} is the maximum current limit from the PEMFC system.

III. Proposed Modifications in Semi-empirical Model

The main deficiencies in the model mentioned above are the use of sensors in obtaining the partial pressure of hydrogen and the assumption that the pressure of oxygen is atmospheric. This may not be the exact case for a PEMFC system. Most commercial PEMFC systems do not have the option to obtain the partial pressure of hydrogen. Besides, the partial pressure of oxygen inside a PEMFC system is not the same as atmospheric pressure. The pressure of vapor inside the PEMFC system varies with the temperature of the PEMFC. This vapor pressure is responsible for the variation in the partial pressure of oxygen and hydrogen. The expression for calculating the partial pressure of oxygen and hydrogen has been given in [10], [22]-[24]. In this paper, the expression for the partial pressure of oxygen and hydrogen given in [24] is considered as it is more accurate, reliable, and simple compared to other expressions.

The expression for calculating the pressure of oxygen P_{O2} from the input pressure at the cathode P_{ca}, which is the atmospheric pressure of air [24], is expressed as:

$$P_{O2} = \frac{P_{ca} - 0.5P_{vap}}{4.76} \quad (17)$$

The constant factor 0.5 is due to the relative humidity of air in an air conditioned room, which is approximately 40% to 50% [25], whereas 4.76 is a general constant.

The expression for calculating the pressure of hydrogen also depends on P_{vap} of the PEMFC system and the inlet pressure of hydrogen P_{an}, which is almost 6 atmospheres in the case of the NEXA 1.2 kW system. The constant C_2 is added in the expression and accounts for the average relative humidity of the cathode and anode.

$$P_{H2} = P_{an} - C_2 P_{vap} \quad (18)$$

Considering these realistic approaches in calculating P_{O2} and P_{H2}, the calculation of no-load voltage will be different from that in [13]. Thus, A_1 and A_2 in (6) must be optimized. R_e is taken as constant in [13]. However, in reality, the electronic resistance is dependent on PEMFC temperature [22]. A new modified expression for electronic resistance can be expressed as:

$$R_e = \frac{D_1}{T} + D_2 \tag{19}$$

The total ohmic resistance R_{ohmic} will be given by:

$$R_{ohmic} = \frac{C_1\left[1 + 0.03I + 0.062\left(\frac{T}{303}\right)^2 I^{2.5}\right]}{\left(\lambda_m - 0.634 - 3I\right)\exp\left(4.18\left(\frac{T-303}{T}\right)\right)} + \frac{D_1}{T} + D_2 \tag{20}$$

The constants D_1 and D_2 should be optimized. Note that R_e only depends on PEMFC temperature. The maximum and minimum limits for various model parameters given in (6)-(8), (12)-(13), (15), (18)-(19) are listed in Table I. The ranges are selected based on previous research findings [10], [13], [14], [24], [26].

TABLE I
MODEL PARAMETERS AND THEIR SUGGESTED RANGES

Parameter	Minimum limit	Maximum limit
A_1	−100	100
A_2	−100	100
α	10^{-4}	5
B_1	10^{-4}	30
B_2	10^{-4}	30
A_{H2O}	10^{-4}	10^{-2}
C_1	10^{-4}	5
C_2	10^{-5}	5
D_1	10^{-5}	500
D_2	10^{-6}	500

The parameters listed in Table I can be extracted by QLSA [27], which is an updated version of the lightening search algorithm (LSA) used in [13] for parameter optimization. QLSA is expected to provide better parameter values in a fast manner as its searching ability is claimed to be superior according to [27]. Nevertheless, for parameter optimization, experiments are required to obtain the output voltage values at specific current and temperature of the PEMFC in order to compare the output voltage of the model with experimental results.

IV. EXPERIMENTS PERFORMED ON PEMFC

The main purpose of the experiments is to collect the variations of output voltage due to the change in the load. During the experiments, other data such as load current and temperate variations are observed and recorded. This information is necessary to optimize the parameters and evaluate the accuracy of the proposed model. In the current work, the experiment has been performed on the NEXA 1.2 kW PEMFC stack system for dynamic variations of load for 2486 s, as shown in Appendix A Fig. A1. The obtained load current, output voltage, and the temperature of PEMFC are shown in Fig. 2. Besides this experiment, system temperature variation due to linear load variation from 0 to 60 A is also conducted.

Figure 2 shows that the variations in load abruptly change from low to high loads at intermittent times. This causes the change of temperature of PEMFC, which is expected to affect the water management of the system. The experimental results provide benchmark values for calculating the error between model output voltage and experimental output voltage. The root mean square error (RMSE) given in (21) is employed as an objective function to be minimized in the optimization.

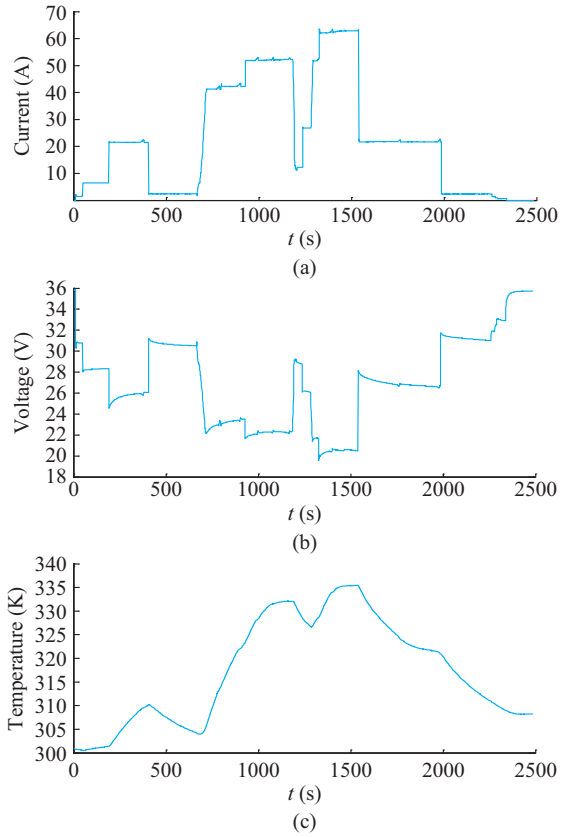

Fig. 2. Experimental results of PEMFC. (a) Current. (b) Voltage. (c) Temperature.

$$RMSE = \sqrt{\frac{\sum (V_{mod} - V_{exp})^2}{T}} \tag{21}$$

where V_{mod} and V_{exp} are the modified and expected voltage drop, respectively.

The procedure for calculating the voltage of the proposed PEMFC semi-empirical model along with RMSE is shown in Fig. 3.

V. PARAMETER EXTRACTION OF PEMFC MODEL USING QLSA

LSA is an optimization technique inspired by the natural phenomena of lightning flashes, which are caused by the propagation of negatively charged particles in space. The idea is first introduced in [27] and extended in [28]. The lightening search process is not continuous. It has regular discrete steps that use a concept called step leader propagation. Projectiles model the progression of step leaders. The three projectiles presented in [27] are: ① transition projectiles, which are the step leader of the main population; ② space projectiles, which strive for the best position as leader; and ③ lead projectiles, which hold the best position among the whole population.

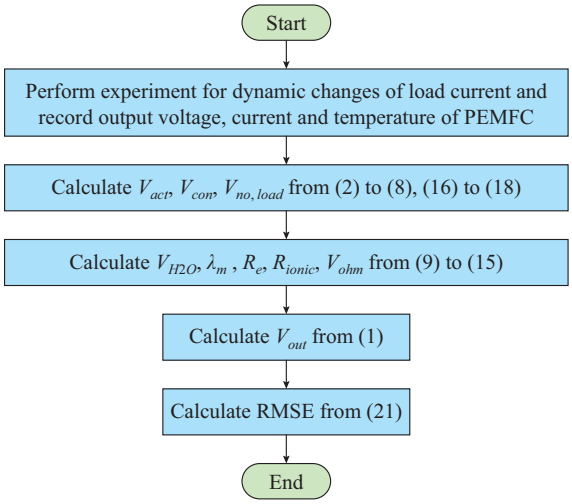

Fig. 3. Model and calculation procedure of RMSE.

In the standard LSA, the search processes for these three projectiles are based on exponential, uniform, and normal probability density functions. However, in QLSA, a quantum physics analogy is used along with special quantum physics equations to improve the search ability.

QLSA searches the new position for its population in order to get the best step leader position. From the beginning, QLSA develops a memory that stores the best positions for step leaders, and these step leaders are called global step leaders $P^t_{i,j,sl}$, which are obtained with the help of objective function evaluation. In this case, the RMSE given in (21) is used. In QLSA, each step leader maintains the best position with a stochastic attractor expressed in (22).

$$p^t_{i,j} = \frac{a^t_{i,j} P^t_{i,j,best} + b^t_{i,j} P^t_{i,j,sl}}{H c^t_{i,j}} \tag{22}$$

where i varies from 1 to N; j varies from 1 to the problem dimension D; t varies from 1 to the maximum number of iterations Z; $a^t_{i,j}$, $b^t_{i,j}$, and $c^t_{i,j}$ are the random numbers uniformly distributed from 0 to 1; $P^t_{i,j,best}$ is the best step leader for every individual population; and H is the scale factor whose typical value is 10.

QLSA is a quantum physics analogy of LSA, and each step leader has quantum behavior with quantum wave equation. For extracting the time and space dependency for the probabilistic model of step leaders to guide their correct movement, quantum physics equations are used with probability density and distribution functions. These equations are explicitly given in [27].

In general, QLSA starts with the initialization of population with $N \times D$ step leaders P. Then, the standard deviation $L_{i,j}$, which is dependent on the mean best position of step leaders, is extracted by:

$$L_{i,j} = 2\beta \left| P_{i,j,mbest} - P_{i,j} \right| \tag{23}$$

where β is the expansion/contraction coefficient, which controls the speed of the algorithm; $P_{i,j,mbest}$ is termed as the mean best position for the step leaders, depending on the objective function and the mean value of the $P_{i,j}$ positions of all step leaders. The formula to calculate $P_{i,j,mbest}$ is:

$$P_{i,j,mbest} = \frac{1}{N} \sum_{i=1}^{N} P_{i,j} \tag{24}$$

β usually controls the speed of convergence of QLSA and can be calculated as:

$$\beta = \beta_o + \frac{(Z-t)(\beta_1 - \beta_o)}{t} \tag{25}$$

where β_1 and β_o are the final and initial values of the coefficient, which are generally set as 1.2 and 0.6, respectively. Finally, the position of step leaders is updated by:

$$P_{i,j,new} = P_{i,j,old} \pm \beta \left| P_{i,j,mbest} - P_{i,j,old} \right| \ln\left(\frac{1}{u_{i,j,new}}\right) \tag{26}$$

where $u_{i,j,new}$ is a random number (uniformly-distributed) between 0 and 1.

The basic implementation steps of the QLSA are shown in Fig. 4.

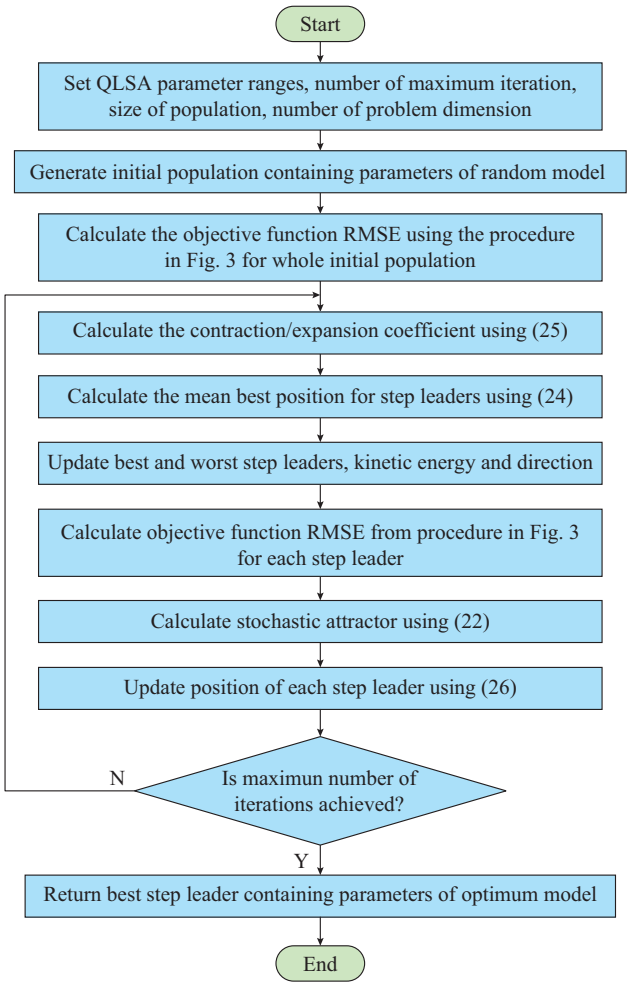

Fig. 4. Basic implementation procedure of QLSA for parameter optimization.

VI. Results and Discussions

A. Model Validation

Initially, the parameters of the proposed PEMFC model are extracted using the procedure given in Section IV, where n and Z are taken as 50 and 400, respectively, and $D = 10$.

Figure 5 shows the convergence characteristic of QLSA in optimizing the PEMFC parameters. At the end of the convergence, the obtained RMSE value is found to be 0.66 with the optimum parameters listed in Table II.

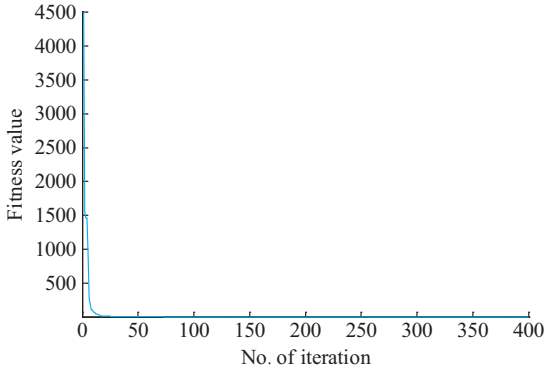

Fig. 5. QLSA convergence characteristics in obtaining model parameters.

TABLE II
OPTIMUM PARAMETER VALUES FOR PROPOSED MODEL

Parameter	Final value
α	1.128955392
B_1	3.924610527
B_2	7.723841989
C_2	1.702027594
A_{H2O}	0.006332088
C_1	3.260638963
D_1	76.102972400
D_2	0.000635566
A_1	0.016836721
A_2	0.860455359

Finally, after extracting the parameters, the model validity is checked by plotting the output voltage of the model with experimental results, as shown in Fig. 6. The proposed model performs well and matches the experimental voltage output.

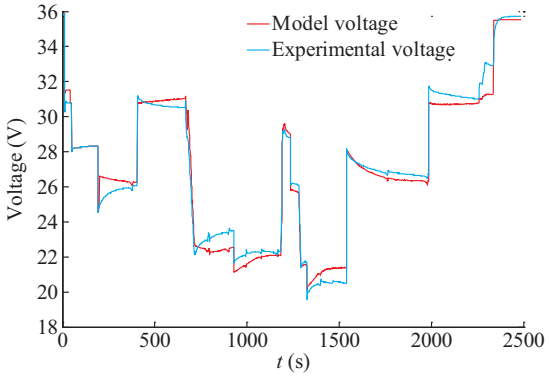

Fig. 6. Comparison of model and experimental voltage.

B. Water Content Analysis for Fault Diagnosis

One of the main advantages of the proposed PEMFC model is the utilization of membrane water content in accessing the output voltage. In this paper, the membrane water content is suggested as the measure of flooding and drying faults in a PEMFC system. The flooding and drying faults in sophisticated systems such as the NEXA 1.2 kW system (educational version) are avoided by incorporating special mechanism to avoid the damage due to misuse of the equipment. The PEMFC model has overheating, under- and over-current and voltage protection, gas sensors and self-humidifying system. However, many other commercial PEMFC systems may not have self-humidifying systems or protection sensors, thus leading to flooding and drying faults.

C. Drying Faults

Since the experiments are performed in an air-conditioned room and the system is equipped with accessories for gas humidification for system protection, it is impossible to create intentional faults. As a result, faults are emulated using the developed model. In addition, the step increases in current from the experiment between 650 s to 950 s is used in the simulations. To analyze the membrane water content, the system temperature has been elevated by 5 K from the normal temperature observed in the experiment. Figure 7 shows the effect of the sudden increase in PEMFC current from 5 A to 40 A and then to 50 A on PEMFC temperature and the membrane water content. Besides, with a 5 K escalation in the temperature, the membrane water content drops significantly, which indicates the effectiveness of the model for drying fault diagnosis.

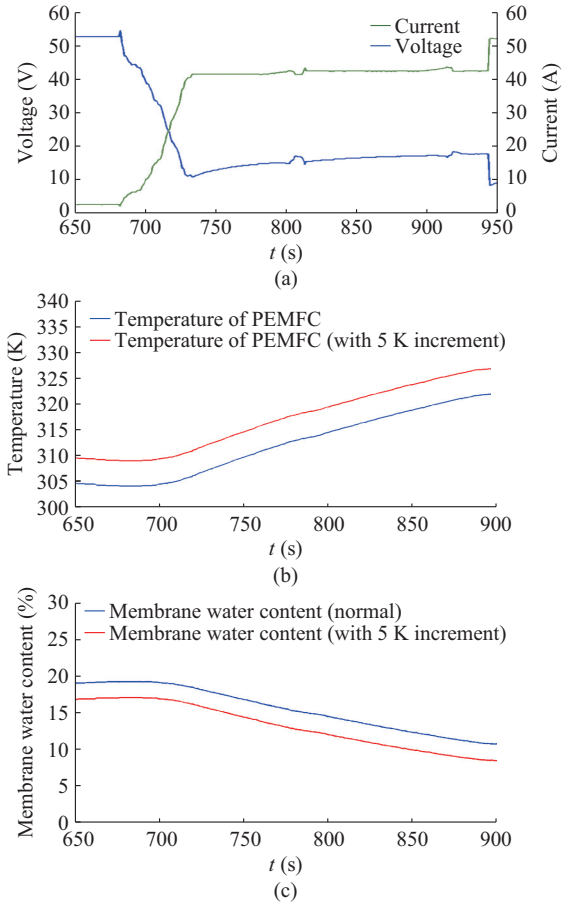

Fig. 7. Drying condition in PEMFC. (a) Current and voltage for step current change in PEMFC as per experiment. (b) 5 K PEMFC temperature increment with step current change via simulation. (c) Membrane water content change for 5 K increment in temperature via simulation.

D. Flooding Faults

In this case, an experiment is performed for a smooth increase in load from 0 A to 60 A to represent high-, medium-, and low-current values. As in [2], a decrease in temperature implies an increase in the water content of the membrane. A decrease in 5 K is simulated compared to the measured experimental temperature and the water content is observed. Figure 8 shows the water content variation with the change in PEMFC temperature due to the load current variations.

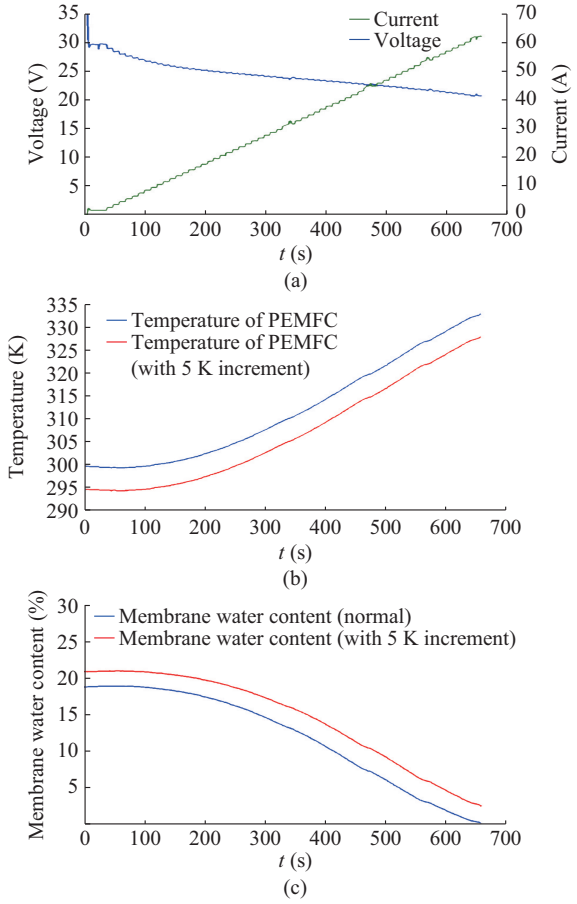

Fig. 8. Flooding condition in PEMFC via simulation. (a) Current and voltage for step current change in PEMFC experimentally. (b) 5 K decrement in PEMFC temperature with step current change via simulation. (c) Membrane water content change for 5 K decrement via simulation.

The vivid elevation in the membrane water content is witnessed with the 5 K decrement in temperature. The membrane water content at high- and low-loading is almost the same, which may not be the case in a real system. Slight variations may occur in real systems for low- and high-loading. The increase in membrane water content for a decrease in 5 K in PEMFC temperature is significant and indicates that the flooding starts to occur with a decrease in temperature.

VII. Conclusion

In this paper, we introduce a new semi-empirical model for a PEMFC stack system with the capability of diagnosing flooding and drying faults. The model requires only the load current and temperature of the PEMFC system, which are commonly available for almost all commercial fuel cells. Thus, the model is considered to be a general model suitable for all PEMFC systems. The membrane water content is extracted as the key model variable factor that could benefit the diagnosis of drying and flooding faults in PEMFC systems. The developed model is dynamic and the equations used are simple to compute. Future research direction should identify the threshold values of membrane water content as an alarm to activate the incorporated fault diagnostic system of PEMFC to prevent drying and flooding related damages to the system. The feature could be very helpful for PEMFC systems without in-built self-humidification accessories.

Appendix A

Fig. A1. NEXA 1.2 kW PEMFC stack system at United Arab Emirates University.

References

[1] E. Breaz, F. Gao, B. Blunier *et al*., "Mathematical modeling of PEMFC stack for real time simulation," in *Proceedings of 2012 IEEE International Conference on Automation, Quality and Testing, Robotics*, Cluj-Napoca, Romania, May 2012, pp. 553-558.

[2] M. Ji and Z. Wei, "A review of water management in polymer electrolyte membrane fuel cells," *Energies*, vol. 2, no. 4, pp. 1057-1106, Nov. 2009.

[3] A. J. del Real, A. Arce, and C. Bordons, "Development and experimental validation of a PEM fuel cell dynamic model," *Journal of Power Sources*, vol. 173, no. 1, pp. 310-324, Nov. 2007.

[4] B. Zhou, W. Huang, Y. Zong *et al*., "Water and pressure effects on a single PEM fuel cell," *Journal of Power Sources*, vol. 155, no. 2, pp. 190-202, Apr. 2006.

[5] M. F. Sheikh, M. Ramzan, S. Khan *et al*., "Review of real-time load of H.A Fibers® grid with distributed fuel cells renewable generation unit," in *Proceedings of 5th International Conference on Renewable Energy Generation and Applications (ICREGA)*, Al Ain, United Arab Emirates, Feb. 2018, pp. 327-331.

[6] S. S. Khan, M. A. Rafiq, H. Shareef *et al*., "Parameter optimization of PEMFC model using backtracking search algorithm," in *Proceedings of 5th International Conference on Renewable Energy Generation and Applications (ICREGA)*, Al Ain, United Arab Emirates, Feb. 2018, pp. 323-326.

[7] I. Labach, O. Rallières, and C. Turpin, "Steady-state semi-empirical model of a single proton exchange membrane fuel cell (PEMFC) at varying operating conditions," *Fuel Cells*, vol. 17, no. 2, pp. 166-177, Feb. 2017.

[8] L. Pisani, G. Murgia, M. Valentini *et al*., "A new semi-empirical approach to performance curves of polymer electrolyte fuel cells," *Journal of Power Sources*, vol. 108, pp. 192-203, Jun. 2002.

[9] J. C. Amphlett, "Performance modeling of the ballard mark IV solid polymer electrolyte fuel cell," *International Journal of Electrochemical Society*, vol. 142, no. 1, pp. 1-8, Jan. 1995.

[10] M. V. Moreira and G. E. da Silva, "A practical model for evaluating the performance of proton exchange membrane fuel cells," *Renewable Energy*, vol. 34, no. 7, pp. 1734-1741, Jul. 2009.

[11] Y. Nalbant, C. O. Colpan, and Y. Devrim, "Development of a one-di-

mensional and semi-empirical model for a high temperature proton exchange membrane fuel cell," *International Journal of Hydrogen Energy*, vol. 43, no. 11, pp. 5939-5950, Mar. 2018.
[12] Y. Hou, M. Zhuang, and G. Wan, "A transient semi-empirical voltage model of a fuel cell stack," *International Journal of Hydrogen Energy*, vol. 32, no. 7, pp. 857-862, May 2007.
[13] S. S. Khan, H. Shareef, A. Wahyudie *et al*., "Novel dynamic semiempirical proton exchange membrane fuel cell model incorporating component voltages," *International Journal of Energy Research*, vol. 42, no. 8, pp. 2615-2630, Apr. 2018.
[14] R. Salim, M. Nabag, H. Noura *et al*., "The parameter identification of the Nexa 1.2 kW PEMFC's model using particle swarm optimization," *Renewable Energy*, vol. 82, pp. 26-34, Oct. 2015.
[15] C. Restrepo, T. Konjedic, A. Garces *et al*., "Identification of a proton-exchange membrane fuel cell's model parameters by means of an evolution strategy," *IEEE Transactions on Industrial Informatics*, vol. 11, no. 2, pp. 548-559, Apr. 2015.
[16] Y. Zhang and J. Jiang, "Bibliographical review on reconfigurable fault-tolerant control systems," *Annual Reviews in Control*, vol. 32, no. 2, pp. 229-252, Dec. 2008.
[17] K. Murugesan and V. Senniappan, "Investigation of water management dynamics on the performance of a Ballard-Mark-V proton exchange membrane fuel cell stack system," *International Journal of Electrochemical Science*, vol. 8, no. 6, pp. 7885-7904, Jun. 2013.
[18] Y. Akimoto and K. Okajima, " Semi-empirical equation of PEMFC considering operation temperature," *Energy Technology Policy*, vol. 1, no. 1, pp. 91-96, Nov. 2014.
[19] A. Atifi, H. Mounir, and A. El Marjani, "Effect of internal current, fuel crossover, and membrane thickness on a PEMFC performance," in *Proceedings of International Renewable and Sustainable Energy Conference (IRSEC)*, Ouarzazate, Morocco, Oct. 2014, pp. 907-912.
[20] S. S. Khan, H. Shareef, and A. H. Mutlag, "Dynamic temperature model for proton exchange membrane fuel cell using online variations in load current and ambient temperature," *International Journal of Green Energy*, vol. 16, no. 5*,* pp. 361-370, Jan. 2019.
[21] Q. Li, W. Chen, S. Liu *et al.*, "Temperature optimization and control of optimal performance for a 300 W open cathode proton exchange membrane fuel cell," *Procedia Engineering*, vol. 29, pp. 179-183, Jan. 2012.
[22] J. Wishart, Z. Dong, and M. Secanell, "Optimization of a PEM fuel cell system based on empirical data and a generalized electrochemical semi-empirical model," *Journal of Power Sources*, vol. 161, no. 2, pp. 1041-1055, Oct. 2006.
[23] J. J. Giner-Sanz, E. M. Ortega, and V. Pérez-Herranz, "Statistical analysis of the effect of the temperature and inlet humidities on the parameters of a PEMFC model," *Fuel Cells*, vol. 15, no. 3, pp. 479-493, Apr. 2015.
[24] J. Zhang, Y. Tang, C. Song *et al*., "PEM fuel cell relative humidity (RH) and its effect on performance at high temperatures," *Electrochimica Acta*, vol. 53, no. 16, pp. 5315-5321, Jun. 2008.
[25] B. Kim, D. Cha, and Y. Kim, "The effects of air stoichiometry and air excess ratio on the transient response of a PEMFC under load change conditions," *Applied Energy*, vol. 138, pp. 143-149, Jan. 2015.
[26] B. Wahdame, D. Candusso, X. Francois *et al*., "Study of a 5 kW PEMFC using experimental design and statistical analysis techniques," *Fuel Cells*, vol. 7, no. 1, pp. 47-62, Feb. 2007.
[27] J. A. Ali, M. A. Hannan, and A. Mohamed, "A novel quantum-behaved lightning search algorithm approach to improve the fuzzy logic speed controller for an induction motor drive," *Energies*, vol. 8, pp. 13112-13136, Nov. 2015.
[28] H. Shareef, A. A. Ibrahim, and A. H. Mutlag, "Lightning search algorithm," *Applied Soft Computing*, vol. 36, pp. 315-333, Nov. 2015.

Saad Saleem Khan received his B.S. and M.S. degrees in electrical engineering from University of Engineering and Technology, Lahore, Pakistan. He completed his Ph.D. degree in 2019 from United Arab Emirates University, Al Ain, United Arab Emirates. He is currently an assistant manager at National Transmission and Dispatch Company Limited, Pakistan. His current research interests include on modelling and fault diagnosis of fuel cell systems.

Hussain Shareef received his B.Sc. degree (Hons.) from Bangladesh Institution of Technology, Dhaka, Bangladesh, M. S. degree from Middle East Technical University, Ankara, Turkey, and Ph. D. degree from Universiti Teknologi Malaysia, Kuala Lumpur, Malaysia, in 1999, 2002, and 2007, respectively. He is currently an Associate Professor in the Department of Electrical Engineering, United Arab Emirates University, Al Ain, United Arab Emirates. His current research interests include power system optimization, power quality, artificial intelligence, and power system automation.

Ahmad Asrul Ibrahim received the B.Eng. and M.Sc. degrees from Universiti Kebangsaan Malaysia, Bangi, Malaysia and the Ph.D. degree from Durham University, Durham, United Kingdom, in 2008, 2012, and 2018, respectively. He is currently a Senior Lecturer in the Department of Electrical, Electronic and Systems Engineering, Universiti Kebangsaan Malaysia. His research interests include distribution system automation, artificial intelligence, renewable energy integrations, and power quality assessment.